Title

Bem1p contributes to secretory pathway polarization through a direct interaction with Exo70p.

Journal

The Journal of cell biology, 207(1)

ISSN

0021-9525

Authors

Liu, Dongmei
Novick, Peter

Publication Date

2014-10-01

DOI

10.1083/jcb.201404122

Peer reviewed

Bem1p contributes to secretory pathway polarization through a direct interaction with Exo70p

Dongmei Liu and Peter Novick

Department of Cellular and Molecular Medicine, University of California, San Diego, La Jolla, CA 92130

The exocyst serves to tether secretory vesicles to cortical sites specified by polarity determinants, in preparation for fusion with the plasma membrane. Although most exocyst components are brought to these sites by riding on secretory vesicles as they are actively transported along actin cables, Exo70p displays actin-independent localization to these sites, implying an interaction with a polarity determinant. Here we show that Exo70p directly and specifically binds to the polarity determinant scaffold protein Bem1p. The interaction involves multiple domains of both Exo70p and Bem1p. Mutations in Exo70p that disrupt its interaction with Bem1, without impairing its interactions with other known binding partners, lead to the loss of actin-independent localization. Synthetic genetic interactions confirm the importance of the Exo70p–Bem1p interaction, although there is some possible redundancy with Sec3p and Sec15p, other exocyst components that also interact with polarity determinants. Similar to Sec3p, the actin-independent localization of Exo70p requires a synergistic interaction with the phosphoinositide PI(4,5)P_2.

Introduction

The ability to direct vesicular traffic to a specific location on the cell surface is critical to a variety of cellular activities such as polarization, ciliogenesis, cytokinesis, migration, and morphogenesis. The exocyst is an octameric complex, comprised of Sec3p, Sec5p, Sec6p, Sec8p, Sec10p, Sec15p, Exo70p, and Exo84p, that is needed to tether secretory vesicles derived from either the Golgi or recycling endosome to specialized sites on the plasma membrane in preparation for exocytic fusion (Munson and Novick, 2006). To fulfill this role, the exocyst must recognize both the vesicles and the appropriate sites at the cell cortex.

In yeast, vesicle recognition by the exocyst is mediated by both the Sec15p subunit, which binds to the vesicle-associated Rab GTPase Sec4p (Guo et al., 1999), and the Sec6p subunit, which binds to the vesicle SNARE Snc2p (Shen et al., 2013). These two subunits, along with Sec5p, Sec8p, Sec10, and Exo84p, travel in association with vesicles as they are actively transported by the type V myosin, Myo2p, along polarized actin cables to sites of cell surface growth (Boyd et al., 2004). Their steady-state localization to these sites is therefore actin dependent.

The localization of the remaining subunits, Sec3p and Exo70p, to exocytic sites is largely actin independent and must therefore reflect an association with polarity determinants that act either upstream or independent of actin (Finger et al., 1998; Boyd et al., 2004). In the case of Sec3p, its actin-independent localization requires an N-terminal domain that interacts with the small GTPases Rho1 and Cdc42, as well as the phosphoinositide PI(4,5)P_2 (Guo et al., 2001; Zhang et al., 2001, 2008; Yamashita et al., 2010). The actin-independent localization of Exo70p is less clearly understood. Exo70p consists of four helical bundles, termed domains A–D, that are linked in series to generate a rod-shaped structure (Dong et al., 2005). Replacement of domain C with a linker has little effect on growth or secretion, but blocks the actin-independent mechanism of Exo70p localization (Hutagalung et al., 2009). Similarly, deletion of the N-terminal region of Sec3p has little effect on growth or secretion, but blocks its actin-independent localization (Guo et al., 2001). Importantly, the combination of these two relatively benign mutations leads to synthetic

Correspondence to Peter Novick: pnovick@ucsd.edu

Abbreviations used in this paper: CBB, Coomassie Brilliant Blue; LatA, Latrunculin A; SC, synthetic complete; TAP, tandem affinity purification; WT, wild type; YPD, yeast extract peptone dextrose.

The Rockefeller University Press $30.00
J. Cell Biol. Vol. 207 No. 1 59–72
www.jcb.org/cgi/doi/10.1083/jcb.201404122

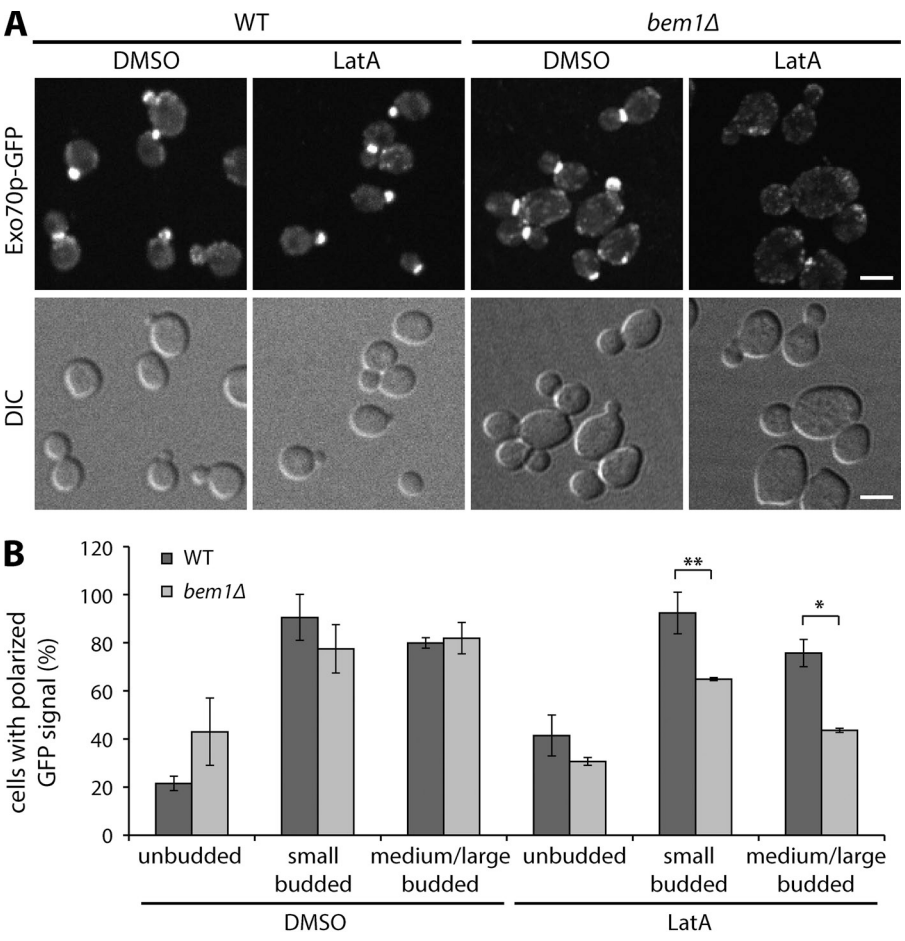

Figure 1. **Exo70p shows localization defects in *bem1Δ* cells.** (A) Yeast cells expressing Exo70p-GFP in WT (NY3052) and a *bem1Δ* mutant (NY3053) were grown to early log phase in SC-URA medium at 25°C. Cells were harvested and treated with DMSO or 200 µM LatA for 10 min and then examined by confocal fluorescence microscopy. Bars, 5 µm. (B) The percentage of cells with polarized GFP signal in unbudded, small-budded, or medium/large-budded cells was quantified. Error bars indicate SD for three separate experiments. For each experiment, 200–300 cells were scored for each strain. *, $P < 0.001$; **, $P < 0.01$; Student's *t* test.

lethality. In fact, this combination of mutations is lethal even in the presence of high copy number suppressors that can bypass a complete deletion of either one of these genes (Hutagalung et al., 2009). Thus, it appears that the N terminus of Sec3p and domain C of Exo70p play a critical role in exocyst function, perhaps relating to their interactions with polarity determinants at the cell cortex. However, they are substantially redundant with each other in this capacity.

Here we explore the actin-independent mechanism of Exo70p localization. Prior studies have shown that Exo70p interacts with Rho3p in its GTP-bound form and that domain C is critical for this interaction (Adamo et al., 1999; Robinson et al., 1999; Dong et al., 2005; He et al., 2007; Hutagalung et al., 2009). However, a more recent study found that the prenyl lipid modified form of Rho3p binds with greater affinity than the unmodified form used in the earlier studies and that this interaction does not require domain C (Wu et al., 2010). Although it is still not clear whether Rho3p plays any essential roles in Exo70p localization, these results imply that domain C must interact with some other actin-independent polarity determinant. We have taken a systematic approach, screening among all the known components that exhibit actin-independent localization to sites of cell surface growth for ones that contribute to the localization of Exo70p. Our studies point to a direct interaction between Exo70p and the polarity determinant scaffold protein Bem1p.

Results

Screen for mutants with Exo70p localization defects

Our previous study showed that deletion of domain C in Exo70p results in a conditional localization defect (Hutagalung et al., 2009). Under normal growth conditions, Exo70ΔdCp-GFP, similar to Exo70p-GFP, localized to bud tips in small-budded cells, isotropically in medium- to large-budded cells, and at the bud necks in cells undergoing cytokinesis. However, upon treatment with Latrunculin A (LatA), a drug that causes depolymerization of actin cables, Exo70ΔdCp-GFP, unlike Exo70p-GFP, was almost completely depolarized except for a small percentage of large-budded cells that maintained the bud neck localization. Therefore, we anticipated that domain C of Exo70p must be important for binding some components that renders its polarized localization actin independent. To identify this component, we performed a directed screen of strains selected from the deletion library, evaluating Exo70p-GFP localization in the presence and absence of LatA. Based on the hypothesis that a protein that recruits and/or anchors Exo70p to polarized cell membrane sites independent of actin must itself target to these sites by an actin-independent mechanism, we assessed Exo70p localization in the following 12 viable yeast deletion strains: *bni4Δ*, *gin4Δ*, *spa2Δ*, *pea2Δ*, *bud6Δ*, *bni1Δ*, *bnr1Δ*, *lte1Δ*, *kel2Δ*, *ste20Δ*, *bem1Δ*, and *boi2Δ* (Ayscough et al., 1997).

We transformed the deletion strains with an integrating vector (NRB880) to tag the endogenous Exo70p copy with GFP at its C terminus. Cells that grew to early log phase in selective synthetic complete (SC) medium were harvested and resuspended in SC medium containing either DMSO or LatA. Among them, *gin4Δ* and *bem1Δ* exhibited decreased polarization of Exo70p in the presence of LatA (Fig. 1 and unpublished data).

Exo70p colocalizes throughout the cell cycle with Bem1p, but not with the septin component Cdc10p

Gin4p is a Nim1-related protein kinase involved in bud growth. It interacts with septins and plays a positive role in assembly of the septin ring (Longtine et al., 1998; Mortensen et al., 2002). It was previously shown that the rat brain sec6/8 (exocyst) complex associates with rat septin proteins (Hsu et al., 1998), therefore it is possible that the defect we observed in *gin4Δ* is through a direct or indirect regulation by the septin complex. However, the exocyst and septin complexes colocalize for only a limited phase of the cell cycle. Typically, the exocyst localizes to bud tips in small-budded cells, isotropically at the cortex of the growing bud in medium- to large-budded cells, and at the bud neck in cells undergoing cytokinesis, whereas septins form a ring structure at the cell cortex ∼15 min before bud emergence, after which the ring broadens to assume the shape of an hourglass around the mother-bud neck. During cytokinesis, the septin cortex splits into a double ring, which eventually disappears (Longtine et al., 1996). We confirmed that Exo70p colocalized with the septin component Cdc10p only at the bud neck during cytokinesis and at the pre-bud site before bud emergence (Fig. S1 B). In contrast, the scaffold protein Bem1p showed extensive colocalization with Exo70p throughout the entire cell cycle, from just before bud emergence until after cytokinesis (Fig. S1 A). The localization of Bem1p-2xmCh was unaffected by the addition of LatA and Exo70p-GFP colocalized with it under this condition (Fig. S1 C; Dyer et al., 2013). Because Exo70p showed more extensive colocalization with Bem1p then with septins and we were looking for a component that regulates Exo70p through direct physical interaction, we have focused here on the role of Bem1p.

Exo70p and Bem1p interact with each other in vitro

Bem1p is a scaffold protein that helps to establish cellular polarity. It contains multiple binding domains that interact with a variety of other members of the intrinsic polarization machinery. It has, from N to C terminus, two SH3 domains, one PX domain, and one PB1 domain. Bem1p interacts with Cdc42p, a Rho-type small GTPase, through the second of its SH3 domains (Bose et al., 2001; Yamaguchi et al., 2007), and with Cdc24p, a guanine-nucleotide exchange factor (GEF) for Cdc42p, through its PB1 domain (Peterson et al., 1994; Butty et al., 2002). Another component of the exocyst complex, Sec15p, was found to interact with Bem1p through its first SH3 domain (France et al., 2006), and the intact exocyst complex was shown to bind to Bem1p (Zajac et al., 2005; France et al., 2006). To test whether Exo70p can directly interact with Bem1p, we expressed and purified

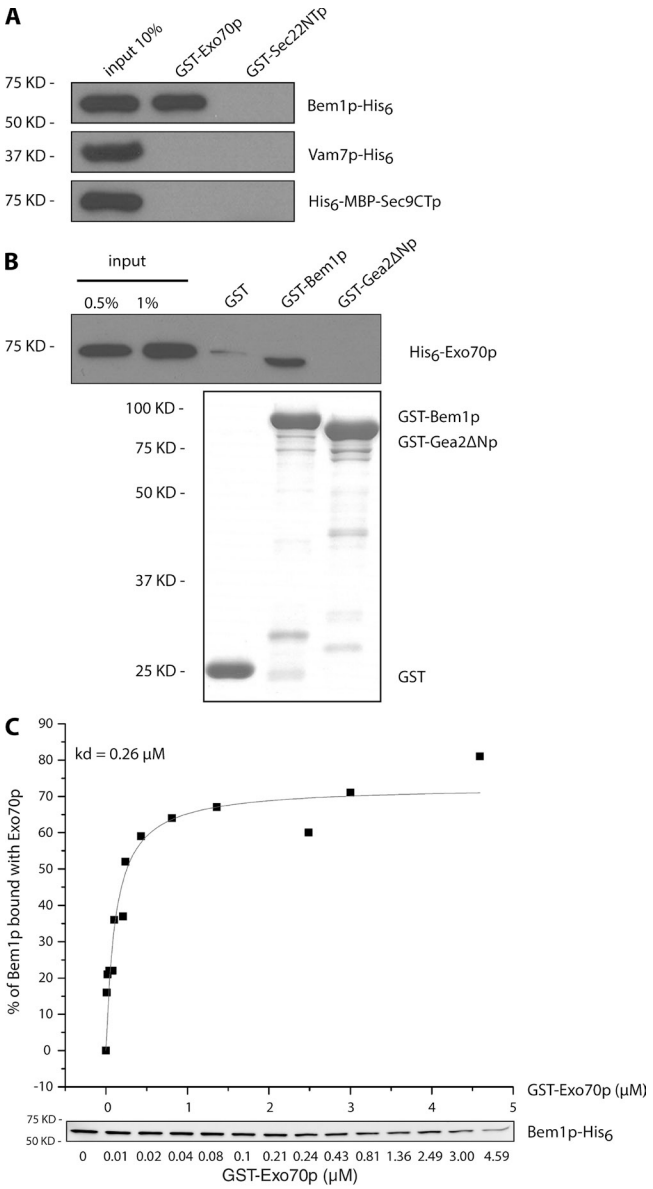

Figure 2. **Exo70p and Bem1p interact with each other in vitro.** (A) GST-Exo70p or GST-Sec22NTp were immobilized on glutathione beads and mixed with purified C-terminal His_6-tagged Bem1p, Vam7p, or N-terminal His_6-MBP–tagged Sec9CTp. Bound proteins were detected with anti-His antibody. (B) GST, GST-Bem1p, or GST-Gea2ΔNp were pre-immobilized on glutathione beads and mixed with purified His_6-Exo70p. Bound GST fusion proteins were detected with CBB staining and associated His_6-Exo70p was detected with anti-His antibody. (C) GST-Exo70p was immobilized on glutathione beads in concentrations ranging from 0 to 4.59 μM. It was then incubated with 25 nM Bem1p-His_6. After pelleting the beads, the amount of Bem1p-His_6 remaining in the supernatant was determined by Western blotting using anti-His antibody and quantified with an Odyssey imaging system. The K_d was calculated with Origin software. The data shown are from a single representative experiment out of three independent repeats.

GST-tagged Exo70p and His_6-tagged Bem1p from bacteria and used them in an in vitro binding assay. As shown in Fig. 2 A, GST-Exo70p binds Bem1p-His_6 efficiently and specifically. Exo70p does not bind the control proteins Vam7p, a t-SNARE containing an N-terminal PX domain (Cheever et al., 2001), and Sec9CTp, containing its two SNARE domains (Brennwald et al., 1994). Furthermore, Bem1p does not bind to a control protein,

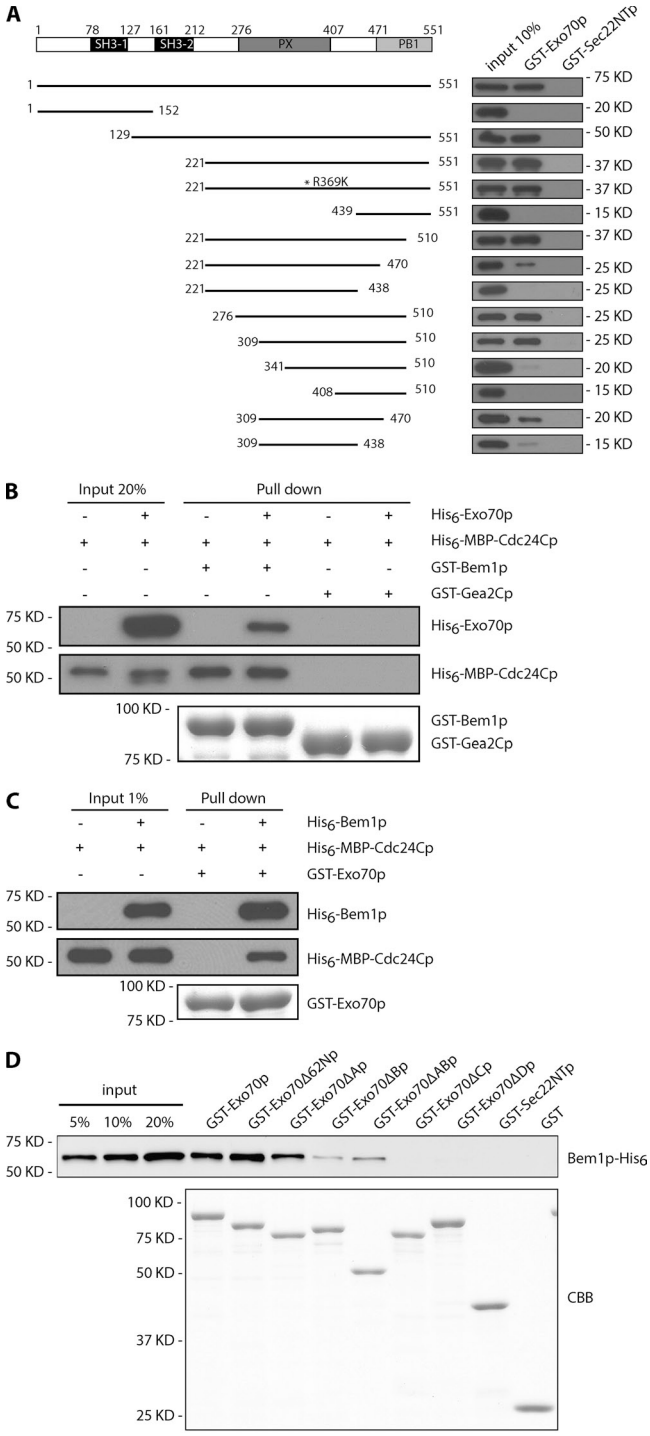

Figure 3. **Mapping the interacting domains of Bem1p and Exo70p.** (A) The PX and PB1 domains of Bem1p are each necessary and together sufficient for interaction with Exo70p. At the upper left is a schematic diagram of the Bem1p protein with SH3-1, SH3-2, PX, and PB1 domains highlighted. In the lower left part, each bar represents either full-length Bem1p or a fragment. Each purified His_6-tagged Bem1p fragment was incubated with glutathione beads with prebound GST-Exo70p or control protein GST-Sec22NTp. Bound Bem1p fragments were detected with anti-His antibody (right). (B) Exo70p does not affect the interaction between Cdc24p and Bem1p. GST-tagged Bem1p or control protein Gea2Cp were immobilized on glutathione beads and then incubated with purified His_6-MBP-Cdc24C in the presence or absence of purified His_6-Exo70p. Bound proteins were detected as described in the Materials and methods. (C) Cdc24p and Exo70p can form a ternary complex with Bem1p. GST-Exo70p was immobilized on glutathione beads and then incubated with purified His_6-MBP-Cdc24C in the presence or absence of purified His_6-Bem1p. Bound proteins were detected as described in the Materials and methods. (D) Each helical bundle domain of Exo70p contributes to the interaction with Bem1p. GST-tagged full-length or domain-deleted Exo70p proteins were immobilized on glutathione beads and then incubated with Bem1p-His_6. Bound proteins were detected as described in the Materials and methods.

Sec22NTp, the N-terminal part of a v-SNARE that acts in ER–Golgi transport (Liu et al., 2004). We also swapped the tags on Exo70p and Bem1p and confirmed that the interaction was not dependent on the orientation of the tags (Fig. 2 B). Using a range of GST-Exo70p concentrations (0–4.59 µM) in equilibrium binding reactions, we determined that the binding of Bem1p is saturable with a K_d of ~0.26 µM (Fig. 2 C). These data indicate that Exo70p and Bem1p interact with each other in vitro in a specific and saturable fashion.

The PX and PB1 domains of Bem1p are each necessary and together sufficient for interaction with Exo70p

To determine which domain of Bem1p is responsible for the interaction with Exo70p, we generated a series of His_6-tagged truncated Bem1p constructs. These fragments were expressed, purified, and used for in vitro binding assays with GST-Exo70p. As shown in Fig. 3 A, the two N-terminal SH3 domains of Bem1p are dispensable for binding because $Bem1^{221\text{-}551}$p interacts with Exo70p as efficiently as full-length Bem1p. Additionally, the first SH3 domain alone ($Bem1^{1\text{-}152}$p) showed no detectable interaction. The PX and PB1 domains together are sufficient for binding Exo70p; however, neither domain alone is sufficient, as indicated by the negative interactions with $Bem1^{221\text{-}438}$p and $Bem1^{439\text{-}551}$p. The PX domain has been determined to be a phosphoinositide-binding module, mediating its membrane targeting. The arginine at 369 is highly conserved in PX domain–containing proteins, and mutation of this conserved arginine to lysine in human $p40^{phox}$ resulted in impaired interaction with PI(3)P (Ago et al., 2001). However, the corresponding mutation in Bem1p ($Bem1^{221\text{-}551R369K}$p) did not interfere with its ability to bind Exo70p. We narrowed down the Exo70p-binding domain of Bem1p to amino acids 309–510, which is both necessary and sufficient. This fragment includes three quarters of the PX domain, half of the PB1 domain, and the region connecting them.

Cdc24p, Bem1p, and Exo70p can form a ternary complex

The PB1 domain of Bem1p is required for Exo70p binding, yet it is also known to bind to the C-terminal PCCR (OPR domain) of Cdc24p (Peterson et al., 1994; Butty et al., 2002). To determine if the Exo70p binding site on Bem1p overlaps with that of Cdc24p, we performed a competition binding study (Fig. 3 B). A fusion protein containing a C-terminal portion of Cdc24 (Cdc24C) was efficiently precipitated by GST-Bem1p, but not by a control protein, GST-Gea2Cp. Addition of a 20-fold excess of Exo70p failed to reduce the precipitation of Cdc24p, which indicates that the Cdc24p and Exo70p binding sites on Bem1p are independent. This suggests that Cdc24p and Exo70p might

be able to form a ternary complex with Bem1p. To test this possibility, Cdc24p was added to GST-Exo70p in the presence or absence of Bem1p. In the absence of Bem1p, no detectable Cdc24p precipitated with GST-Exo70p; however, in the presence of Bem1p, both Bem1p and Cdc24p were precipitated with Exo70p (Fig. 3 C). Thus, a ternary Exo70p–Bem1p–Cdc24p complex can be formed.

Bem1p interacts more strongly with Exo70p than with Sec15p

We previously showed that another subunit of the exocyst complex, Sec15p, interacts directly with Bem1p in vitro, and that it is the C-terminal domain of Sec15p (740–910) and N-terminal SH3 domain of Bem1p that mediate the interaction (France et al., 2006). Since we identified a direct interaction of Bem1p with Exo70p, we compared the relative strengths of these two interactions side by side. As shown in Fig. S2, Exo70p appears to interact more efficiently with Bem1p than with Sec15Cp. Because different regions of Bem1p are responsible for each interaction, Bem1p may be able to bind both subunits of the exocyst complex at the same time.

All four helical bundle domains of Exo70p contribute to its interaction with Bem1p

Next we mapped the domains of Exo70p that are responsible for the interaction with Bem1p. Exo70p consists of an N-terminal region of 62 amino acids followed by four helical bundles, termed domains A–D. We generated four GST-tagged expression constructs, each with a different domain deleted and replaced with a linker. We also made a construct that removes the N-terminal 62 amino acids because it has previously been shown that Exo70Δ62Np is fully functional in vivo and has better solubility than full-length Exo70p when expressed in bacteria (Dong et al., 2005). We immobilized each truncated GST-Exp70p construct on glutathione beads and examined their ability to bind to Bem1p. We found that Exo70Δ62Np interacts with Bem1p at a comparable or even higher level than full-length Exo70p (Fig. 3 D). However, each domain deletion either weakly (Exo70ΔdAp), dramatically (Exo70ΔdBp), or completely (Exo70ΔdCp and Exo70ΔdDp) reduced the binding to Bem1p (Fig. 3 D). These results indicate that all four helical bundle domains of Exo70p contribute to the interaction with Bem1p and that Exo70p domains C and D play essential roles.

Exo70M26p shows dramatically reduced binding to Bem1p

Because we previously found that yeast cells expressing Exo70ΔdCp as the sole copy of Exo70p displayed a localization defect upon treatment with LatA (Hutagalung et al., 2009), we proposed that Exo70p may interact with a polarity determinant through its C domain. Consistent with the hypothesis that this component is Bem1p, data described above indicate that Exo70p domain C is essential for Bem1p binding (Fig. 3 D). To extend this correlation, we sought to isolate mutations within the C domain that disrupt binding to Bem1p. Surface-exposed charged residues within the C domain were systematically mutated to alanine either one at a time or as small patches. These mutations were numbered from 1 to 15 in order (Fig. 4 A), and constructs expressing the GST-tagged Exo70p mutants were generated. We refer to these mutant proteins as Exo70M1p–Exo70M15p. We subsequently found that the initial "Exo70M13p" construct had two unintended mutations within domain B (S196F and L246S), which had been introduced during PCR mutagenesis. This mutant was therefore renamed Exo70M28p (Fig. 4 B). We also reverted the two extra mutations back to the wild-type (WT) sequence to generate bona fide Exo70M13p. These GST-tagged Exo70 mutants were then expressed and immobilized on glutathione beads for in vitro binding assays. Among these mutants, only Exo70M28p and Exo70M15p showed reduced binding with Bem1p (Fig. 4 C, lane 3 and 11; Fig. 4 D; and unpublished data). To identify a more potent mutation that completely disrupts the interaction, we tested a variety of constructs that combined Exo70p mutations and thereby isolated Exo70M26p and Exo70M30, both of which showed only a minimal level of binding to Bem1p (Fig. 4 C, lane 13–14; and Fig. 4 D). As shown in Fig. 4 E, Exo70M26p, which combines mutations within both C domain (Exo70M22p) and B domain (Exo70M25p), is more potent than either single domain mutation in its effects on Bem1p binding, and this difference is more dramatic at higher concentrations (Fig. 4 E). This result together with data shown in Fig. 3 D demonstrates that multiple domains of Exo70p contribute to Bem1p binding.

Exo70M26p loses actin-independent polarization

We examined the localization of the Exo70p mutants that most dramatically diminished the interaction with Bem1p. We introduced these mutations into the *EXO70* genomic locus and fused GFP to their C termini. The mutant yeast were grown to early log phase, harvested, and treated with either DMSO or LatA before examination by fluorescence confocal microscopy. Consistent with our prior findings, Exo70ΔdC-GFPp localization is sensitive to LatA treatment (Hutagalung et al., 2009; Fig. 5). The percentage of small-budded cells with bud-tip localization was reduced from 92% in WT to 22% in *exo70ΔdC*, whereas ∼45% of medium- to large-budded *exo70ΔdC* cells maintained isotropic localization in daughter cells or bud-neck localization in contrast to 76% in WT cells. We examined the Exo70Mp-GFP localization in five of the mutants described in the previous paragraph: *M20*, *M22*, *M25*, *M26*, and *M30*. Among them, Exo70M20p and Exo70M22p showed a normal level of binding to Bem1p (Fig. 5 and unpublished data), and Exo70M25p showed a moderate reduction, whereas Exo70M26p and Exo70M30p showed the most extensively impaired interaction with Bem1p. The results establish a good correlation between Bem1p binding in vitro and Exo70Mp-GFP polarized localization in vivo: the mutants that retain the ability to interact with Bem1p, such as *exo70M20*, *exo70M22*, and *exo70M25*, largely maintained actin-independent polarized localization, especially for small-budded cells. A partial reduction in binding with Bem1p was associated with decreased polarization in medium/large-budded cells. However, the mutants that almost completely lost the ability to bind Bem1p, such as *exo70M26* and *exo70M30*, also failed to exhibit polarized localization in the presence of LatA

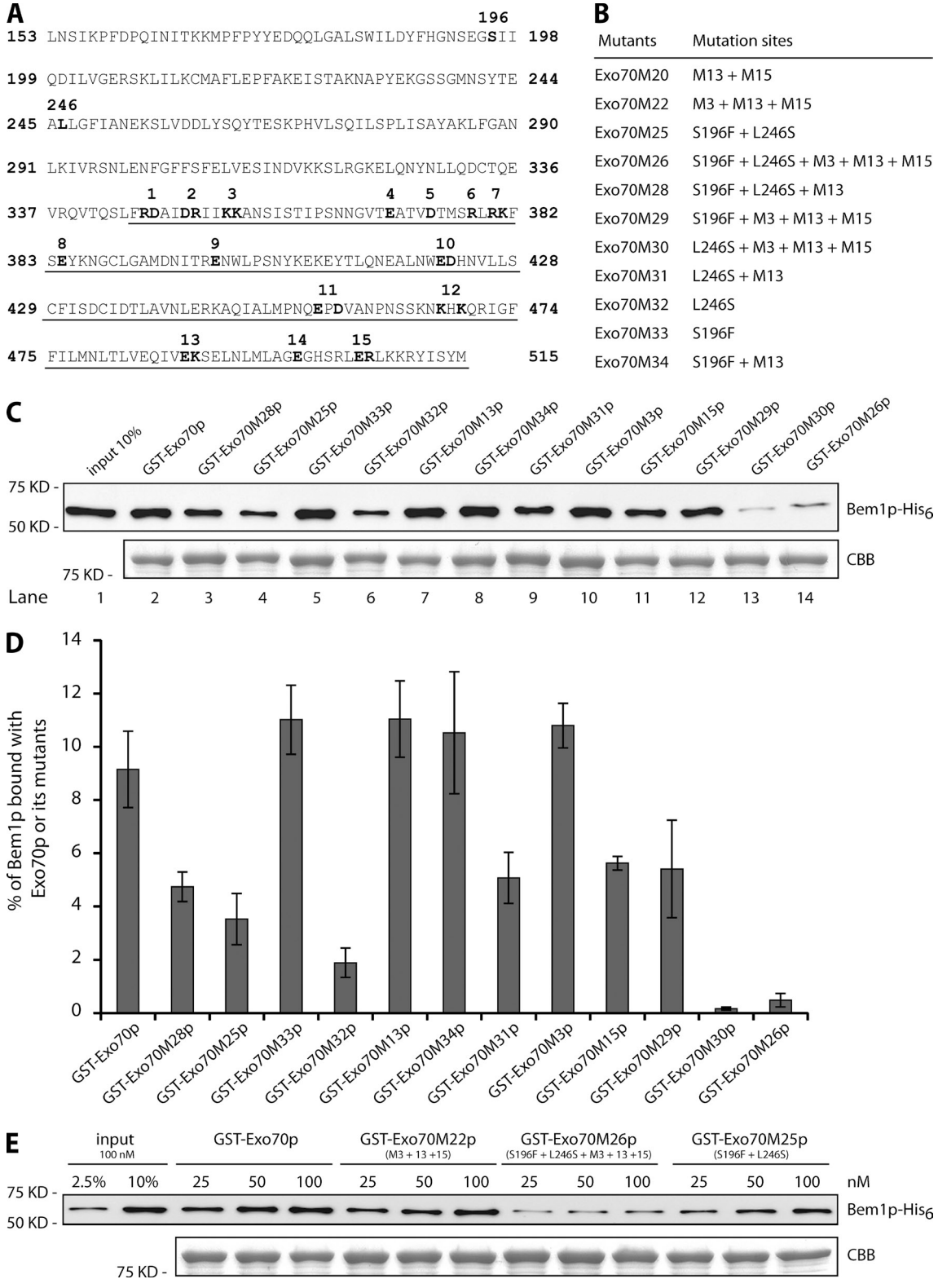

Figure 4. **Exo70M26p is severely impaired in binding to Bem1p.** (A) Amino acid sequence of Exo70p domains B and C from 153 to 515. The sequence of domain C is underlined. Surface-exposed charged residues within the C domain are indicated by bold text. They were systematically mutated to alanine either one at a time or in small patches. These mutation sites are numbered from 1 to 15 in order. Two unintentional mutations were found within domain B in our original M13 construct (renamed M28), serine at position 196 was mutated to phenylalanine (S196F), and leucine at position 246 was mutated to serine (L246S). (B) Some of the single mutation sites were combined and given a new name, shown on the left column of the table. (C) GST-tagged WT Exo70p or mutants were immobilized on glutathione beads and incubated with Bem1p-His_6. Bound proteins were detected as described in the Materials and methods. (D) The percentage of Bem1p bound to Exo70p WT or mutants was quantified. Error bars represent SD, $n = 3$. (E) The interactions between Bem1p-His_6 and GST-Exo70p WT or three mutants were tested at three different concentrations of Bem1p: 25 nM, 50 nM, and 100 nM. Bound proteins were detected as mentioned in the Materials and methods.

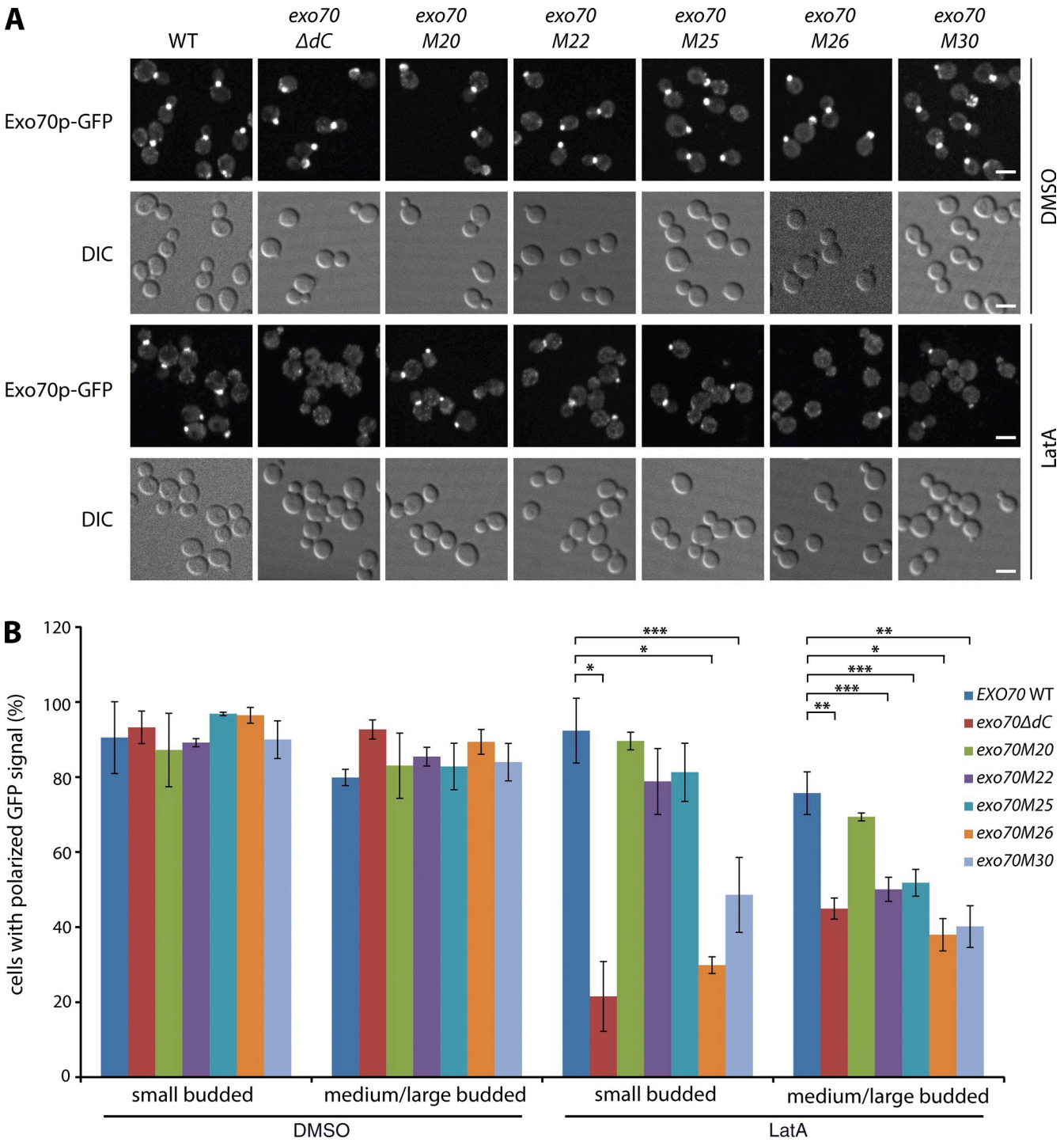

Figure 5. **Exo70M26p loses actin-independent polarization.** (A) Yeast cells expressing WT Exo70p-GFP (NY3052) or various mutants (NY3054, NY3056, NY3057, NY3058, NY3059, and NY3060) were grown to early log phase in synthetic medium at 25°C. Cells were harvested and treated with DMSO or 200 µM LatA for 10 min and then examined by confocal fluorescence microscopy. Bars, 5 µm. (B) The percentage of cells with polarized GFP signal in small-budded or medium/large-budded cells was quantified. Error bars indicate SD for three separate experiments. For each experiment, 200–300 cells were scored for each strain. *, $P < 0.001$; **, $P < 0.002$; ***, $P < 0.005$; Student's *t* test.

(Fig. 5). Mutant *exo70M26* displayed a severe defect similar to that of *exo70ΔdC*, with 30% localized to the bud tip in small-budded cells and 38% localized isotropically in the daughter cells or bud-neck localization in medium/large-budded cells (Fig. 5). The *exo70M26* mutation had no effect on the localization of Bem1-2xmCh in the presence of LatA (Fig. S1 D). The correlation between Bem1p binding and Exo70p polarized localization strongly supports the hypothesis that Bem1p contributes to Exo70p polarization through a direct interaction.

Table 1. **Summary of genetic interactions between *exo70* mutants or *bem1Δ* and *sec3ΔN*, *sec3-2*, or *sec15-1***

Mutants	*sec3ΔN*	*sec3-2*	*sec15-1*
exo70ΔdC	Synthetic lethal	Synthetic lethal	Synthetic lethal
exo70M3	No effect	Synthetic sick	Not available
exo70M20	No effect	Synthetic sick	Synthetic sick
exo70M22	No effect	Synthetic sick	Not available
exo70M25	No effect	Not available	Not available
exo70M26	Synthetic lethal	Synthetic lethal	Synthetic lethal
exo70M30	No effect	Synthetic sick	Synthetic lethal
bem1Δ	Synthetic lethal	Not available	Synthetic lethal

exo70M26 is synthetically lethal with late-blocked *sec* mutants

To further explore the effects of these *exo70* mutations in vivo, we assessed genetic interactions between the various *exo70* mutations and mutations in *sec3* or *sec15*. Sec3p and Exo70p are the only two subunits of the exocyst exhibiting actin-independent localization (Boyd et al., 2004). We previously showed that *exo70ΔdC* is synthetically lethal with *sec3ΔN*. Neither mutant alone has significant effects on growth or secretion, but each results in the loss of actin-independent localization, which suggests that the N terminus of Sec3p and domain C of Exo70p play a critical but largely redundant role in exocyst function (Hutagalung et al., 2009). Sec15p is the other exocyst component that has been shown to directly interact with Bem1p, and the interaction requires the C terminus of Sec15p, which is truncated in the *sec15-1* mutant (France et al., 2006). We crossed *sec3ΔN*, *sec3-2*, *and sec15-1* to each of seven *exo70 mutants* (*exo70ΔdC*, *exo70M3*, *exo70M20*, *exo70M22*, *exo70M25*, *exo70M26*, and *exo70M30*) with only a few exceptions (Table 1). Consistent with our previous results, *exo70ΔdC* is synthetically lethal with *sec3ΔN* and *sec3-2* (Hutagalung et al., 2009). Here, we show that it is also synthetically lethal with *sec15-1* (Table 1). *exo70M26* not only mirrored the localization defect of *exo70ΔdC*, it also exhibited a similar pattern of genetic interactions (Fig. S3 A and Table 1). Other than *exo70M26*, no other mutants showed any synthetic defect with *sec3ΔN*. This includes *exo70M30*, which, like *exo70M26*, showed both a localization defect and impaired interaction with Bem1p. These results suggest that, in addition to their localization defects, *exo70M26* and *sec3ΔN* may have lost another essential role that was not lost in *exo70M30*. Similarly, other than *exo70M26*, no other point mutants showed any synthetic defect with *sec3-2* at 25–30°C. However, synthetic effects were observed at 34°C, with a range of weak (*M3*, *M20*) to strong effects (*M22* and *M30*). Apparently, cumulative effects result from additional mutation sites (Table 1 and Fig. S3 B, top). In addition to being synthetically lethal with *exo70M26*, *sec15-1* was also synthetically lethal with *exo70M30* (Fig. S3 A). The synthetic lethality of the bem1-binding–deficient *exo70* alleles with *sec15-1* and *sec3ΔN* predicts that loss of *BEM1* itself should lead to synthetic lethality with *sec15-1* and *sec3ΔN*, and this prediction was confirmed (Fig. S3 A and Table 1).

We also extended the comparison between *exo70M26* and *exo70ΔdC* by crossing *exo70M26* with ts alleles of all of the post-Golgi-blocked *sec* mutants (Table 2). With only a few exceptions, the two *exo70* mutations exhibited similar patterns of genetic interactions, being lethal in combination with *sec2-41*, *sec3-2*, *sec4-8*, *sec9-4*, *sec10-2*, and *sec15-1* (Fig. S3 A). In the case of *sec6-4*, a synthetic negative interaction was observed, and in the case of *sec8-9*, synthetic lethality was observed in combination with *exo70ΔdC*, yet no synthetic effect was seen with *exo70M26.* Conversely, in the cases of *sec1-1* and *sec5-24*, synthetic negative interactions were seen with *exo70M26*, whereas no effect was seen with *exo70ΔdC* (Table 2 and Fig. S3 B). Thus, *exo70M26* appears to have lost most, but not all functions of domain C, as well as some additional function that can be attributed to domain B.

Table 2. **Summary of genetic interactions between *exo70M26* or *exo70ΔdC* with late-blocked *sec* mutants**

Mutants	*exo70M26*	*exo70ΔdC*[a]
sec1-1	Synthetic sick	No effect
sec2-41	Synthetic lethal	Synthetic lethal
sec3-2	Synthetic lethal	Synthetic lethal
sec4-8	Synthetic lethal	Synthetic lethal
sec5-24	Synthetic sick	No effect
sec6-4	No effect	Synthetic sick
sec8-9	No effect	Synthetic lethal
sec9-4	Synthetic lethal	Synthetic lethal
sec10-2	Synthetic lethal	Synthetic lethal
sec15-1	Synthetic lethal	Synthetic lethal

[a]The genetic interaction data between *exo70ΔdC and sec* mutants have been published previously (Hutagalung et al., 2009).

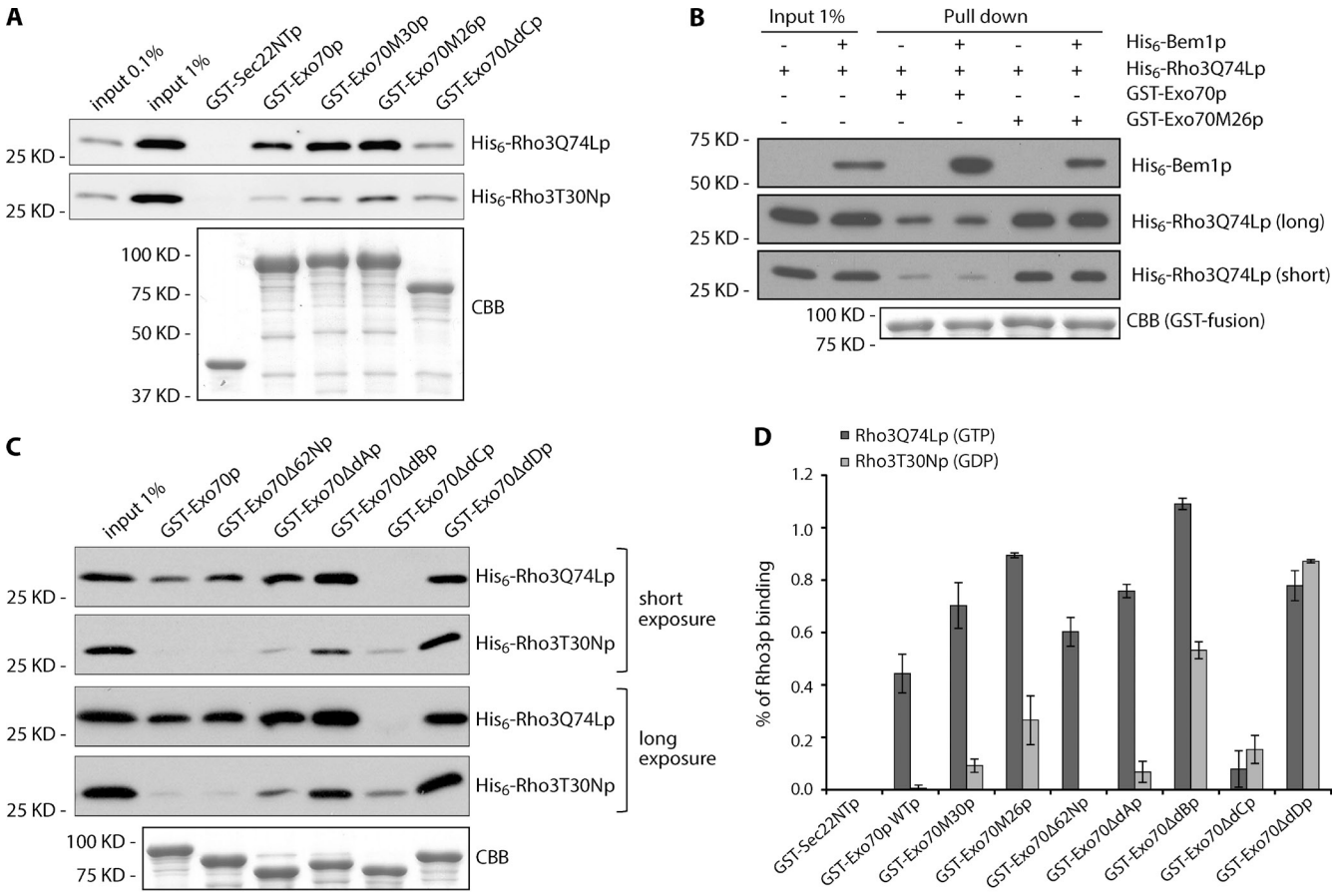

Figure 6. **Bem1p-binding–deficient mutations in Exo70p do not impair its interactions with Rho3p-GTP.** (A) GST-tagged WT Exo70p or mutant proteins (M26, M30, and ΔdC) were immobilized on glutathione beads and then incubated with yeast lysate expressing His_6-Rho3Q74Lp (GTP-locked form) or His_6-Rho3T30Np (GDP-locked form). Bound proteins were detected as described in the Materials and methods. (B) Bem1p does not compete with Rho3p for Exo70p binding. GST-tagged WT Exo70p or M26 mutant proteins were immobilized on glutathione beads and then incubated with yeast lysate expressing His_6-Rho3Q74Lp (GTP-locked form) in the presence or absence of purified His_6-Bem1p. Bound proteins were detected as described in the Materials and methods. Two different exposures (labeled long and short) of the Rho3p blot are shown. (C) Exo70p single domain deletion mutants with an N-terminal GST-tag were pre-immobilized on glutathione beads and incubated with yeast lysate expressing His_6-Rho3Q74Lp or His_6-Rho3T30Np. Bound proteins were detected as described in the Materials and methods. Two different exposures of the Rho3p blots are shown. (D) The percentage of His_6-Rho3Q74Lp or His_6-Rho3T30Np bound to Exo70p WT or mutants was quantified. Error bars represent SD; $n = 3$.

Bem1p-binding–deficient mutations in Exo70p do not impair its interactions with other known binding partners

Exo70p is a subunit of an octameric protein complex (TerBush et al., 1996). To explore whether Exo70M26p or Exo70M30p interfere with exocyst complex assembly, we introduced these mutations into the genomic *EXO70* locus and added a tandem affinity purification (TAP) tag to its C terminus. Yeast cells were harvested and subjected to TAP to isolate components associated with Exo70p WT or mutants. As shown in Fig. S4 A, both mutants pulled out the same set of exocyst subunits as WT, and in similar amounts. The only apparent change in the two mutant precipitates is a shift in the mobility of the Exo70Mp-CBP band itself, which may reflect the change of several charged residues to alanine.

Several groups have reported on the interaction of Exo70p with the GTPase Rho3p and mapped the interaction to the internal C domain (Dong et al., 2005; He et al., 2007; Hutagalung et al., 2009). These studies were performed with unprenylated proteins purified from bacteria. It was later reported by Wu et al. (2010) that binding of prenylated Rho3p from yeast lysates is not dependent on domain C. We examined Rho3p binding to the Exo70p mutants using the approach of Wu et al. (2010), except we added a His_6 tag at the N terminus of Rho3p to facilitate detection instead of using Rho3p antibody to detect untagged Rho3p. We found that neither mutation diminished binding to GTP-locked Rho3p and that they actually bound even more than WT (Fig. 6, A and D). Because this binding reaction used yeast lysate containing both Bem1p and Rho3p, the increased binding of Rho3p by Exo70p mutants that cannot bind Bem1p could reflect a reduction in competition for a common binding site on Exo70p. To explore this possibility, we performed a competition experiment in which we tested the effect of Bem1p addition on the efficiency of precipitation of Rho3Q74Lp with either GST-Exo70p or GST-Exo70M26p (Fig. 6 B). Addition of Bem1p had no effect on the binding of Rho3p to either Exo70p or Exo70M26p. As in previous experiments, we observed greatly reduced binding of Bem1p and significantly enhanced binding of Rho3p to Exo70M26p relative to Exo70p. These observations indicate that the Rho3p binding site on Exo70p does

not overlap with the Bem1p binding site. The enhanced binding of Rho3p to Exo70M26p might reflect a more accessible binding site for this ligand.

We also tested the interaction of Rho3p with each of the single domain deletion mutants of Exo70p (Fig. 6, C and D). The results obtained with prenylated Rho3p expressed in yeast are consistent with what we found previously with nonprenylated Rho3p expressed in bacteria (Dong et al., 2005). In both cases, Exo70p domain C appears to be the major domain responsible for Rho3p binding. Using the method of Wu et al. (2010), we also tested the interaction of Exo70M26p and Exo70M30p with another known binding partner, Cdc42p. Again, these mutations did not interfere with Cdc42p binding (unpublished data).

A previous study demonstrated that Exo70p is anchored to the cell membrane in part through an interaction of its positively charged C-terminal tail with the phosphoinositide $PI(4,5)P_2$ (He et al., 2007). To rule out the possibility that the observed localization defects of Exo70M26p or Exo70M30p are caused by a disruption of $PI(4,5)P_2$ binding, we performed a liposome binding study. We found that both purified mutant proteins precipitate to some extent even in the absence of liposomes; however, we observed increased precipitation in the presence of $PI(4,5)P_2$ liposomes (Fig. S4 B). By subtracting the background precipitation, we found that these mutants showed similar levels of $PI(4,5)P_2$-dependent sedimentation as WT (Fig. S4 C). Consistent with a prior report (He et al., 2007), Exo70M16p ($Exo70^{R595A}p$), a point mutation in the D domain, dramatically decreased $PI(4,5)P_2$-dependent sedimentation (Fig. S4, B and C). We also tested whether this $PI(4,5)P_2$-binding–deficient mutation has any effect on Bem1p binding. As shown in Fig. S4 D, Exo70M16p interacted with Bem1p as well as WT Exo70p.

Because the Exo70M26p and Exo70M30p mutations did not interfere with exocyst complex formation or binding to Rho3p, Cdc42p, and $PI(4,5)P_2$, they appear to specifically disrupt the interaction with Bem1p. However, the possible involvement of other unknown components cannot be excluded.

exo70 mutants deficient in Bem1p binding are nearly normal in secretory function

Invertase and Bgl2 are delivered to the cell surface through two distinct populations of secretory vesicles, and both populations are blocked in all 10 of the original complementation groups of late *sec* mutants (Harsay and Bretscher, 1995). To study secretion in the Bem1p-binding–deficient mutants, we performed invertase and Bgl2 secretion assays as well as direct visualization of secretory vesicles by thin section electron microscopy. Mutants *exo70M26* and *exo70M30* showed the same level of Bgl2 secretion as WT at both 25°C and 37°C (Fig. S5 B). Less than a 2% reduction in the efficiency of invertase secretion was observed in both mutants compared with WT (Fig. S5 A). We also examined *exo70M26* mutant cells by EM. Consistent with the minor invertase secretion defect, *exo70M26* yeast cells accumulated ∼11.7 secretory vesicles per cell section in contrast to ∼ 2.4 in WT cells (Fig. S5 C). This phenotype is similar to that of *exo70ΔdC*, as previously reported (Hutagalung et al., 2009). The mild secretion defect and modest vesicle accumulation phenotype of the Bem1p binding–deficient *exo70* mutants suggested that a *bem1* mutant would display similar defects. As shown in Fig. S5 (A and C), *bem1Δ* cells exhibited a 6% reduction in invertase secretion and about a fivefold increase in the number of secretory vesicles relative to WT.

Discussion

Here we establish a direct and specific interaction between Exo70p, a subunit of the exocyst tethering complex, and Bem1p, a scaffold protein involved in polarity establishment. We further demonstrate that this interaction allows Exo70p to concentrate at exocytic sites independent of actin function. Because actin is required for the polarized delivery of secretory vesicles, this result implies that by binding Bem1p, Exo70p can be recruited to these sites independent of vesicular traffic. Although loss of this interaction has no strong effect on growth or secretion in otherwise normal cells, synthetic effects are seen in combination with defects in Sec3p or Sec15p, reflecting the importance of this interaction for exocyst function.

The results presented here are consistent with our prior model of exocyst function in which six of the subunits are recruited to the surface of secretory vesicles through interactions with both the Rab GTPase Sec4p and the vSNARE Snc1/2p, and then brought to sites of exocytosis by actin- and myosin-mediated active vesicle transport (Guo et al., 1999; Boyd et al., 2004; Shen et al., 2013). The other two subunits, Sec3p and Exo70p, can be recruited to exocytic sites by binding to components of the polarity establishment machinery, independent of actin-mediated vesicle traffic. The recruitment of Sec3p to these sites requires the interaction of an N-terminal region with Cdc42 or Rho1 (Guo et al., 2001; Zhang et al., 2001) as well as $PI(4,5)P_2$ (Zhang et al., 2008; Yamashita et al., 2010). Exo70p interacts with Rho3p (Adamo et al., 1999; Robinson et al., 1999; Dong et al., 2005; He et al., 2007; Hutagalung et al., 2009) and Cdc42p; however, it has been argued that these interactions serve to activate Exo70p rather than recruit it to exocytic sites (Wu et al., 2010). We have identified Exo70p mutants that are unable to bind to Bem1p and have lost the actin-independent mechanism for localization, but still bind to the other partners, including the other subunits of the exocyst, Rho3p, Cdc42p, and $PI(4,5)P_2$. These findings support the proposal that the interaction of Exo70p with Bem1p is required for its recruitment and confirm that the interactions with Rho3p and Cdc42p are not sufficient for this function. Analogous to the synergistic roles of Rho GTPases and $PI(4,5)P_2$ in the polarized localization of Sec3p, the actin-independent localization of Exo70p requires interactions with both Bem1p and $PI(4,5)P_2$ because the disruption of either Bem1p or $PI(4,5)P_2$ binding is detrimental to this function (Fig. 5; He et al., 2007).

Exo70p forms an extended rod-shaped structure consisting of a series of four helical bundles (Dong et al., 2005). All four bundles contribute to the interaction with Bem1p, with domains C and D being the most critical. Our analysis of surface charge to alanine mutations supports the hypothesis that multiple domains of Exo70p contribute to Bem1p binding, as combining mutations in domain B and C had a stronger effect on binding

than the mutations in either domain alone. Bem1p is also a multidomain protein, and both the PX and PB1 domains are required for Exo70p binding. In total, our results suggest that Bem1p binds along the length of the Exo70p rod. The interaction of Exo70p with Bem1p does not interfere with the ability of Bem1p to bind Cdc24p, and we show evidence for an Exo70p–Bem1p–Cdc24p ternary complex. Furthermore, Bem1p binding does not interfere with the interaction of Exo70p and Rho3p. We have previously established that Bem1p also binds the exocyst subunit Sec15p (France et al., 2006). That interaction involves the C terminus of Sec15p and the N-terminal SH3 domain of Bem1p. Because different domains of Bem1p are involved in binding Sec15p and Exo70p, it is possible that both exocyst subunits interact with Bem1p at the same time, thereby increasing the avidity of the assembled complex.

In mammalian epithelial cells, Exo70p was the only exocyst subunit found to correctly localize when overexpressed (Yeaman et al., 2004), which suggests that it might directly recognize a landmark at the cell cortex. Although there is no clear mammalian counterpart of Bem1p, there are many proteins containing PX or PB domains and it will be important to determine which, if any, of them are involved in Exo70 recruitment.

Materials and methods

Plasmid and strain construction

The plasmids and yeast strains used in this study are listed in Tables S1–S3. To generate the GST-Exo70p expression vector (NRB1508), full-length *EXO70* was PCR amplified from WT yeast genomic DNA with BamHI and NotI sites on either side. It was then double digested with BamHI–NotI and inserted into pGEX4T2 (SFNB806) linearized with the same two enzymes. A similar approach was used to construct Exo70 without 62N (NRB1509), domain A (NRB1510), domain AB (NRB1512), domain D (NRB1514), and Bem1 (NRB1543). pGEX4T2-Exo70ΔdB (NRB1511) was constructed by PCR using pRS306-Exo70ΔdB-Adh1t as a template. It was then cloned into StuI–XhoI double-digested pGEX4T2-Exo70 full length by gap repair. Similarly, pGEX4T2-Exo70ΔdC (NRB1513) was constructed by PCR using pET46-Exo70ΔdC as a template. Targeted mutation in the C domain of Exo70 was performed by site-directed mutagenesis.

To generate the His_6-MBP-Exo70p expression vector (NRB1561), full-length *EXO70* was PCR amplified from WT yeast genomic DNA with BamHI and NotI sites on either side. It was then double digested with BamHI–NotI and inserted into pSV282 linearized with the same two enzymes. A similar approach was used to generate the different His_6-MBP-tagged Exo70 mutants, except using the corresponding GST-tagged vector as a PCR template.

To generate the His_6-MBP-$Cdc24^{781\text{-}854}$p (His_6-MBP-Cdc24C) expression vector (NRB1582), the C-terminal 74 codons of Cdc24 were PCR amplified from WT yeast genomic DNA with BamHI and NotI sites on either side. It was then double digested with BamHI–NotI and inserted into pSV282 linearized with the same two enzymes.

To generate C-terminal His_6-tagged fusion protein expression vectors, different fragments of Bem1 or Vam7 were PCR amplified and cloned into NdeI–XhoI linearized pET29a (SFNB338) by gap repair.

To construct yeast strains expressing GFP-tagged *EXO70* with various mutations, pRS305- or pRS306-based HemiZAP vectors were first constructed by cloning the *EXO70* C-terminal fragment (711–1,869 bp in the case of *M3*, *M20*, and *M22* or 233–1,869 bp in the case of *M25*, *M26*, and *M30*) fused with GFP into pRS305-Adh1t (JCB83) or pRS306-Adh1t (NRB879). Mutations were generated by site-directed mutagenesis. HemiZAP vectors were then linearized with BglII or BclI and transformed into the WT yeast strain BY4741 or *bem1Δ* (NY3051) to integrate into the *EXO70* locus. To construct yeast strains expressing TAP-tagged *EXO70* with mutations, pRS305 based HemiZAP vectors were first constructed by replacing the GFP tag in pRS305-Exo70M26(M30)-GFP-Adh1t with the TAP tag. It was then linearized with BclI and transformed into the WT yeast strain BY4741 to integrate into the *EXO70* locus. Transformants were PCR amplified and sequence verified to confirm the introduction of the *exo70* mutations into its WT locus and thereby its function as a sole copy of the gene. To make a HemiZAP vector with *sec3ΔN* under control of its own promoter (NRB1574), 772 bp of *SEC3* 5′ UTR plus the *SEC3* start codon and *SEC3* coding sequence from amino acids 321–1,336 were sequentially cloned into pRS303-Adh1t XhoI–SacII sites. It was then linearized with SpeI and transformed into the diploid yeast strain NY2277, which has only one copy of *SEC3*, to integrate into the *SEC3* promoter locus. The haploid yeast strain with *sec3ΔN* integrated into the *sec3Δ* chromosome (NY3064) was obtained by tetrad dissection and verified by PCR analysis. To make a HemiZAP vector with N-terminal His_6-tagged Rho3Q74L or Rho3T30N under Gal promoter control (NRB1577, NRB1578), WT *RHO3* was first PCR amplified and recombined into NdeI–BamHI double digested pET15b by gap repair. Rho3Q74L and Rho3T30N were generated by site-directed mutagenesis. Using these vectors as a template, His_6-Rho3Q74L or His_6-Rho3T30N were PCR amplified and inserted into BglII–PstI double-digested pNB529. They were then linearized with BstEII and transformed into WT yeast strain NY1211 to integrate into the *LEU2* locus (NY3068, NY3069). To construct a yeast strain coexpressing Exo70p-GFP/Bem1p-2xmCherry (NY3073), HemiZAP vector pRS305-Bem1-2xmCherry-Adh1t (NRB1580) was first constructed by cloning the *BEM1* C-terminal fragment (925–1,653 bp) into pRS305-2xmCherry-Adh1t (NRB1579) double digested with XhoI–XbaI. It was then linearized with BstAPI and transformed into a yeast strain expressing Exo70p-GFP (NY3052) to integrate into the *BEM1* locus. To construct a yeast strain coexpressing Exo70p-3xGFP/Cdc10p-2xmCherry (NY3074), HemiZAP vector pRS305-Cdc10-2xmCherry-Adh1t (NRB1581) was first constructed by cloning the *CDC10* C-terminal fragment (384–966 bp) into pRS305-2xmCherry-Adh1t (NRB1579) double digested with XhoI–XbaI. It was then linearized with BglII and transformed into a yeast strain expressing Exo70p-3xGFP (NY2515) to integrate into the *CDC10* locus.

Protein expression and purification from *Escherichia coli*

pGEX4T2-, pET21a-, pET29a-, and pSV282-related expression vectors were transformed into Rosetta cells to express GST-, His_6-, or His_6-MBP–tagged fusion proteins. Fresh Luria broth (LB) medium was inoculated with a 1:100 dilution of an overnight culture and incubated with shaking at 37°C. When the OD_{600} reached 0.6–0.7, the culture was kept on ice for 30 min, then IPTG was added to a final concentration of 0.1 mM to induce target protein expression. The culture was further incubated at 16°C with shaking overnight before harvest. To purify proteins with a GST tag, the cell pellet was resuspended with 1× PBS, pH 7.4, 1 mM EDTA, 1 mM DTT, and 1 mM PMSF, and sonicated for a total of 2 min, alternating 10 s on and 10 s off. Triton X-100 was then added to a 0.5% final concentration and the crude lysate was further incubated on a nutator at 4°C for 15 min. Cell debris was removed by centrifugation at 15,000 rpm for 30 min at 4°C. Cell lysate was incubated with glutathione–Sepharose 4B beads (GE Healthcare) at 4°C for 2 h and washed five times with lysis buffer containing 0.1% Triton X-100. To purify proteins with a His_6 tag, the cell pellet was resuspended with 1× PBS, 160 mM NaCl, 15 mM imidazole, pH 8.0, 5 mM β-ME, and 1 mM PMSF. Cleared cell lysate was incubated with Ni-NTA agarose beads (QIAGEN) and washed five times with lysis buffer containing 0.1% Triton X-100 and 25 mM imidazole. When necessary, purified proteins were eluted from corresponding affinity purification beads with 20 mM glutathione, 100 mM Tris, pH 8.0, 300 mM NaCl (for GST-tagged fusion proteins), or 1× PBS, 160 mM NaCl, 400 mM imidazole, pH 8.0, and 5 mM β-ME (for His_6-tagged fusion proteins). Protein concentration was estimated by SDS-PAGE and Coomassie Brilliant Blue (CBB) staining using BSA as a standard.

To prepare His_6-MBP-Exo70 WT and mutants for liposome-binding experiments, His_6-MBP-Exo70p or mutants were eluted from Ni-NTA beads with 1× PBS, 160 mM NaCl, 400 mM imidazole, pH 8.0, and 5 mM β-ME. Purified proteins were then applied on PD MiniTrap G-10 columns to exchange buffer to 50 mM Hepes, pH 7.2, 120 mM KAc, 1 mM DTT, and 5% glycerol.

In vitro binding assays

Exo70p–Bem1p binding assay. GST-Exo70p WT, fragments, or mutants, pre-immobilized on glutathione beads, were incubated with purified C-terminal His_6-tagged WT Bem1, its fragments, or mutants, in binding buffer (1× PBS, pH 7.4, 1 mM DTT, 0.1% Triton X-100, and 1 mg/ml BSA). The total volume for each binding reaction was 200 µl. The final concentrations for GST-Exo70p and Bem1p-His_6 were 0.15 µM and 0.1 µM, respectively. The binding mixture was incubated at room temperature for 1 h followed by five washes with binding buffer without BSA. Bound proteins were resolved

with Laemmli sample buffer and subjected to CBB staining to detect GST fusion proteins and Western blotting with mouse monoclonal anti-His antibody (AM1010a, 1:1,000; Abgent) to detect associated His_6-tagged proteins.

Competition assay of Exo70p and Cdc24Cp for Bem1 binding. 0.2 µM GST-Bem1p or GST-Gea2p (control), pre-immobilized on glutathione beads, was incubated with purified 0.2 µM His_6-MBP-Cdc24Cp in the presence or absence of 4 µM His_6-Exo70p. To test whether Cdc24p, Bem1p, and Exo70p can form a ternary structure, 0.2 µM GST-Exo70p, pre-immobilized on glutathione beads, was incubated with purified 1 µM His_6-MBP-Cdc24Cp in the presence or absence of 1 µM His_6-Bem1p. The binding mixture was incubated at 4°C for 2 h followed by five washes with binding buffer. Bound proteins were detected as described in the Exo70p–Bem1p binding assay section.

Exo70p-Rho3p binding assay. The Exo70p-Rho3p binding assay was adapted from the procedure of Wu et al. (2010). Yeast strains (NY3068 and NY3069) were grown in YP medium with 2% raffinose to mid-log phase (OD ~1). Expression of N-terminal His_6-tagged Rho3Q74Lp or Rho3T30Np was induced by adding galactose to a final 2% concentration and grown at 25°C for five more hours. Yeast cells were pelleted and lysed with lysis buffer (20 mM Tris-HCl, pH 7.5, 120 mM NaCl, 10 mM $MgCl_2$, 1 mM DTT, 1 mM PMSF, 2× protease inhibitor cocktail, and 1% Tween 20). 1 ml of yeast lysate from 50 OD cells were incubated with 0.1 µM GST-Exo70p WT, fragments, or mutants, which were pre-immobilized on glutathione beads, for 2 h at 4°C. The beads were washed five times with lysis buffer. Bound proteins were detected as described in the Exo70p–Bem1p binding assay section. The Exo70p-Cdc42p binding assay was performed similarly with yeast strains (BY1054 and BY1055) except that Cdc42p was detected by Cdc42 mouse monoclonal antibody (1:200; provided by P. Brennwald, University of North Carolina School of Medicine, Chapel Hill, NC).

Competition assay of Bem1p and Rho3p for Exo70p binding. 0.07 µM GST-Exo70p or GST-Exo70M26p, pre-immobilized on glutathione beads, was incubated with yeast lysate expressing His_6-Rho3Q74L in the presence or absence of 0.7 µM purified His_6-Bem1p. The binding mixture was incubated at 4°C for 2 h followed by five washes with binding buffer. Bound proteins were detected as described in the Exo70p–Bem1p binding assay section.

Determination of the dissociation equilibrium constant (K_d) for the Exo70p–Bem1p interaction

The K_d for the Exo70p–Bem1p interaction was determined as described previously (Pollard, 2010). In brief, 0–4.59 µM of GST-Exo70p, pre-immobilized on glutathione beads, was mixed with 25 nM Bem1p-His_6 in 200 µl of binding buffer (1× PBS, pH 7.4, 1 mM DTT, and 0.1% Triton X-100) and incubated at room temperature for 1 h. The binding mixture was centrifuged at 5,000 rpm for 1 min. The amount of Bem1p-His_6 remaining in the supernatant was determined by Western blotting using anti-His antibody (AM1010a; Abgent) and quantified with an Odyssey imaging system. The K_d was calculated with Origin software.

Fluorescence microscopy and quantitative localization analysis

Yeast strains harboring a GFP-tag at the C terminus of WT Exo70p or its mutants were grown at 25°C to early log phase (OD_{600} 0.4–0.6) in selective SC medium. 1 ml of cells were pelleted and resuspended in the same medium. Cells were further subjected to treatment with DMSO alone or with 200 µM LatA in DMSO as described previously (Hutagalung et al., 2009). Fluorescence imaging was performed as described previously (Shen et al., 2013). In brief, images were acquired with a 63× oil immersion objective lens (Plan Apochromat 63×/1.4 NA oil DIC lens; Carl Zeiss) on a spinning disc confocal microscopy system (Yokogawa Electric Corporation), which includes a microscope (Observer Z1; Carl Zeiss) equipped with an electron multiplying charge-coupled device (CCD) camera (QuantEM 512SC; Photometrics). Excitation of GFP or mCherry was achieved using 488-nm argon and 568-nm argon/krypton lasers, respectively. For each sample, a z stack of 17–20 slices with a 300-nm slice distance was generated. Images were analyzed using AxioVision software 4.8 (Carl Zeiss). To quantify the polarization of WT Exo70p-GFP or its mutants, for each strain, three independent clones were tested and at least 200 cells for each clone were scored. When the GFP signal was mainly detected in the bud tip of small-budded cells, an isotropic distribution over the surface of the growing bud of medium/large-budded cells, or the bud neck of large-budded cells, these cells were scored as polarized. Other cells were scored as depolarized.

Growth test

Yeast cells were grown overnight in yeast extract peptone dextrose (YPD) medium to stationary phase. Cells were washed once with sterile water and diluted to an OD_{600} of 5. In the case of yeast strains with the *sec3-2* mutation, for incubation at 34°C, cells were spotted in twofold serial dilutions starting with OD_{600} at 5. For incubation at 25°C and 30°C, cells were spotted in twofold serial dilutions starting with OD_{600} at 0.01. For all other yeast strains, cells were spotted in fivefold serial dilutions starting with OD_{600} at 5.

TAP tag purification of exocyst protein complex

Exo70p WT or mutants were C-terminally fused with a TAP tag (WT, NY3065; *M26*, NY3066; *M30*, NY3067). The TAP complex was purified as described by De Craene et al. (2006) with minor modifications. Basically, 2 liters of yeast cells (grown at 25°C to OD_{600} 1.5) were resuspended in 10 ml of lysis buffer (20 mM Pipes, pH 6.8, 150 mM NaCl, 1 mM EDTA, 1 mM PMSF, 1× protease inhibitor cocktail, and 10 mM β-ME). The cell suspension was split into twelve 2-ml screw cap tubes (Thermo Fisher Scientific) with 2 g zirconia/silica 0.5-mm beads (Biospec Products, Inc.), prewashed with ice-cold lysis buffer without protease inhibitor, and shaken twice for 3 min with a 1-min interval. NP-40 was added to a 0.5% final concentration and the lysate was incubated at 4°C for 15 min. The lysate was then spun at 20,000 *g* for 30 min. The resulting supernatant was then incubated with Immunoglobulin G (IgG)-Sepharose beads (GE Healthcare) at 4°C for 3 h. After TEV protease cleavage, released proteins were then incubated with Calmodulin beads (Agilent Technologies) at 4°C for 2 h. The final elute was concentrated, mixed with Laemmli sample buffer, and subjected to SDS-PAGE and silver staining to detect the exocyst subunits.

Liposome preparation and sedimentation assay

The liposome preparation and sedimentation assay was performed as described previously (Stalder et al., 2013). 1-Palmitoyl-2-oleoyl-sn-glycero-3-phospho-L-serine (POPS), 1,2-dipalmitoyl-sn-glycero-3-phosphoethanolamine (DPPE), 1,2-dipalmitoylsn-glycero-3-phosphocholine (DPPC), and PI(4,5)P_2 were from Avanti Polar Lipids, Inc. All liposomes contained 20 mol% DPPE and 30 mol% POPS, with or without 5 mol% PI(4,5)P_2. The remaining lipid was DPPC. Lipids in chloroform were mixed in a pear-shaped glass flask. The flask was attached to a rotary evaporator and immersed in a water bath at 33°C for 5 min before evaporation. A lipid film was produced by rapid evaporation of chloroform under vacuum. The lipid film was then resuspended in 50 mM Hepes and 210 mM sucrose, pH 7.2 (4 mM lipids). The resuspension was subjected to five freeze/thaw cycles and was extruded through a polycarbonate filter with a pore size of 0.1 µm. Liposomes were rebalanced in a buffer containing 50 mM Hepes, pH 7.2, 120 mM KAc, 1 mM $MgCl_2$, and 1 mM DTT. Purified His_6-MBP-Exo70p WT or mutants (0.4 µM) were precleared at 55,000 rpm for 15 min to remove any aggregates and then mixed with 0.4 mM liposomes in a total volume of 70 µl. The binding mixture was incubated at room temperature for 15 min. After ultracentrifugation at 55,000 rpm for 15 min at 20°C, the supernatant was removed and mixed with 1/3 volume of 4× SDS sample buffer. The pellet was resuspended in the same volume of 1× SDS sample buffer as the total volume of sample buffer-treated supernatant. Proteins in the supernatant and pellet were visualized by SDS-PAGE followed by CBB staining. The amount of the proteins in the supernatant and pellet was determined by ImageJ software.

Invertase secretion assay

The invertase secretion assay was performed as described by Shen et al. (2013). Basically, yeast cells were grown at 25°C in YPD medium (5% glucose) overnight to early log phase (0.3–0.8 OD/ml). 0.5 OD cells were transferred to a 15-ml Falcon tube, pelleted, washed once with 1 ml of 10 mM NaN_3, and kept on ice. This was the 0 h sample. Another 0.5 OD cells were washed once with sterile water, resuspended in 1 ml of YPD (0.1% glucose), and incubated at 37°C with shaking for 1 h. Cells were pelleted, resuspended in 1 ml of 10 mM NaN_3, and kept on ice. This was the 1 h sample. For each 0 h and 1 h sample, the external invertase was measured directly. The internal invertase was measured after cells were converted into spheroplast and lysed with 0.5 ml of 0.5% Triton X-100. The percentage of invertase secretion was calculated by [Ext (1 h) − Ext (0 h)]/{[Ext (1 h) − Ext (0 h)] + [Int (1 h) − Int (0 h)]}.

Bgl2 secretion assay

The Bgl2 secretion assay was performed as described by Kozminski et al. (2006) with minor modification. In brief, 40 ml of yeast cells were grown at 25°C in YPD medium overnight to early log phase (~0.3 OD/ml). About 4.5 OD cells were transferred into a new flask. Two sets were prepared for each strain. One set was incubated at 25°C and the other set was incubated at 37°C with shaking for 90 min. Cell cultures from both

temperatures were then harvested by centrifugation at 900 *g* for 5 min. Cell pellets were resuspended in 1 ml of ice-cold 10 mM NaN_3 and 10 mM NaF, followed by a 10-min incubation on ice. The suspension was transferred to microfuge tubes, pelleted, and resuspended in 1 ml of fresh prespheroplasting buffer (100 mM Tris-HCl, pH 9.4, 50 mM β-mercaptoethanol, 10 mM NaN_3, and 10 mM NaF). After a 15-min incubation on ice, cells were pelleted and washed with 0.5 ml of spheroplast buffer (50 mM KH_2PO_4-KOH, pH 7.0, 1.4 M sorbitol, and 10 mM NaN_3). Cells were resuspended in 1 ml of spheroplast buffer containing 167 µg/ml zymolyase 100T (Nacasai Tesque Inc.). Cells were incubated in a 37°C water bath for 30 min. Spheroplasts were then pelleted at 5,000 *g* for 10 min, and 100 µl of the supernatant was transferred into a new tube and mixed with 34 µl of 4× SDS sample buffer. This was the external pool. All the remaining supernatant was removed and the pellet (spheroplast) was resuspended in 100 µl of 2× SDS sample buffer. This was the internal pool. 20 µl for each internal pool samples (20% of total) and 27 µl for each external pool samples (2% of total) were loaded on a 15% SDS-PAGE gel. Bgl2p was visualized by Western blotting with anti-Bgl2p rabbit polyclonal antibody at 1:1,000 dilution (provided by W. Guo, University of Pennsylvania, Philadelphia, PA). Loading control Adh1p was visualized by Western blotting with anti-Adh1p rabbit polyclonal antibody (AB1202; EMD Millipore) at 1:10,000 dilution.

Electron microscopy

Yeast cells expressing WT Exo70p (NY3065), Exo70M26p (NY3066) with TAP tag, or deficient of Bem1p (NY3051) were grown at 25°C in YPD medium and processed for electron microscopy as described by Chen et al. (2012). In brief, yeast cells were grown overnight to early log phase ($OD_{600\ nm}$ = 0.3–0.6) at 25°C. Approximately 10 $OD_{600\ nm}$ units of cells were collected using a 0.22 µm filter apparatus, washed with 10 ml of 0.1 M cacodylate, pH 6.8, resuspended in 10 ml of fixative (0.1 M cacodylate and 4% glutaraldehyde, pH 6.8), and incubated for 1 h at room temperature before the cells were stored overnight at 4°C. The next day, the fixed cells were washed twice with 50 mM KPi, pH 7.5, and then resuspended in 2 ml of 50 mM KPi, pH 7.5, buffer containing 0.25 mg/ml Zymolyase 100T. Cells were then incubated for 40 min at 37°C in a water bath with gentle shaking. After the incubation, the cells were washed twice with ice-cold 0.1 M cacodylate buffer using a 0.22 µm filter apparatus, and resuspended in 1.5 ml of cold 2% OsO4 in 0.1 M cacodylate buffer. Cells were then incubated for 1 h on ice in a hood, washed with water, and then incubated in 2% uranyl acetate (UrAc) for 1 h at room temperature. Cells were dehydrated using a series of ethanol washes, and incubated overnight in Spurr resin. Cells were embedded in fresh Spurr resin and baked at 80°C for at least 24 h. Sections were stained with lead citrate and uranyl acetate, and images were acquired using a transmission electron microscope (Tecnai G2 Spirit; FEI) equipped with a CCD camera (UltraScan 4000; Gatan).

Online supplemental material

Fig. S1 shows localization of Exo70p, Bem1p, and Cdc10p through the cell cycle. Fig. S2 shows that Bem1p interacts more strongly with Exo70p than with Sec15p. Fig. S3 shows genetic interactions between *exo70* and late-blocked *sec* mutants. Fig. S4 shows that Bem1p-binding–deficient mutations in Exo70p do not impair its interactions with other exocyst components or $PI(4,5)P_2$. Fig. S5 shows that *exo70* mutants deficient in Bem1p binding have only a minor secretory defect. Table S1 lists the plasmids used for bacteria expression. Table S2 lists the plasmids used for yeast transformation. Table S3 lists the yeast strains used in this study. Online supplemental material is available at http://www.jcb.org/cgi/content/full/jcb.201404122/DC1. Additional data are available in the JCB DataViewer at http://dx.doi.org/10.1083/jcb.201404122.dv.

We thank Y. Jones from the laboratory of M. Farquhar for preparation of samples for electron microscopy, the laboratory of S. Dowdy for sharing equipment, and D. Stalder for assistance in liposome preparation (Department of Cellular and Molecular Medicine, University of California at San Diego). We also thank P. Brennwald (Department of Cell Biology and Physiology, University of North Carolina School of Medicine) for *cdc42* yeast strains and antibodies. We acknowledge W. Guo (Department of Biology, University of Pennsylvania) for the Bgl2 antibody. We are also grateful to A. Hutagalung (Verdezyne, Inc.) for initiating this project and to J. Coleman (Department of Cell Biology, Yale University School of Medicine) and E. France (Department of Biological and Environmental Sciences, Georgia College & State University) for technical assistance.

This work was funded by a grant (GM35370) from the National Institutes of Health to P. Novick.

The authors declare no competing financial interests.

Submitted: 23 April 2014
Accepted: 3 September 2014

References

Adamo, J.E., G. Rossi, and P. Brennwald. 1999. The Rho GTPase Rho3 has a direct role in exocytosis that is distinct from its role in actin polarity. *Mol. Biol. Cell*. 10:4121–4133. http://dx.doi.org/10.1091/mbc.10.12.4121

Ago, T., R. Takeya, H. Hiroaki, F. Kuribayashi, T. Ito, D. Kohda, and H. Sumimoto. 2001. The PX domain as a novel phosphoinositide- binding module. *Biochem. Biophys. Res. Commun.* 287:733–738. http://dx.doi.org/10.1006/bbrc.2001.5629

Ayscough, K.R., J. Stryker, N. Pokala, M. Sanders, P. Crews, and D.G. Drubin. 1997. High rates of actin filament turnover in budding yeast and roles for actin in establishment and maintenance of cell polarity revealed using the actin inhibitor latrunculin-A. *J. Cell Biol.* 137:399–416. http://dx.doi.org/10.1083/jcb.137.2.399

Bose, I., J.E. Irazoqui, J.J. Moskow, E.S. Bardes, T.R. Zyla, and D.J. Lew. 2001. Assembly of scaffold-mediated complexes containing Cdc42p, the exchange factor Cdc24p, and the effector Cla4p required for cell cycle-regulated phosphorylation of Cdc24p. *J. Biol. Chem.* 276:7176–7186. http://dx.doi.org/10.1074/jbc.M010546200

Boyd, C., T. Hughes, M. Pypaert, and P. Novick. 2004. Vesicles carry most exocyst subunits to exocytic sites marked by the remaining two subunits, Sec3p and Exo70p. *J. Cell Biol.* 167:889–901. http://dx.doi.org/10.1083/jcb.200408124

Brennwald, P., B. Kearns, K. Champion, S. Keränen, V. Bankaitis, and P. Novick. 1994. Sec9 is a SNAP-25-like component of a yeast SNARE complex that may be the effector of Sec4 function in exocytosis. *Cell*. 79:245–258. http://dx.doi.org/10.1016/0092-8674(94)90194-5

Butty, A.C., N. Perrinjaquet, A. Petit, M. Jaquenoud, J.E. Segall, K. Hofmann, C. Zwahlen, and M. Peter. 2002. A positive feedback loop stabilizes the guanine-nucleotide exchange factor Cdc24 at sites of polarization. *EMBO J.* 21:1565–1576. http://dx.doi.org/10.1093/emboj/21.7.1565

Cheever, M.L., T.K. Sato, T. de Beer, T.G. Kutateladze, S.D. Emr, and M. Overduin. 2001. Phox domain interaction with PtdIns(3)P targets the Vam7 t-SNARE to vacuole membranes. *Nat. Cell Biol.* 3:613–618. http://dx.doi.org/10.1038/35083000

Chen, S., P. Novick, and S. Ferro-Novick. 2012. ER network formation requires a balance of the dynamin-like GTPase Sey1p and the Lunapark family member Lnp1p. *Nat. Cell Biol.* 14:707–716. http://dx.doi.org/10.1038/ncb2523

De Craene, J.O., J. Coleman, P. Estrada de Martin, M. Pypaert, S. Anderson, J.R. Yates III, S. Ferro-Novick, and P. Novick. 2006. Rtn1p is involved in structuring the cortical endoplasmic reticulum. *Mol. Biol. Cell*. 17:3009–3020. http://dx.doi.org/10.1091/mbc.E06-01-0080

Dong, G., A.H. Hutagalung, C. Fu, P. Novick, and K.M. Reinisch. 2005. The structures of exocyst subunit Exo70p and the Exo84p C-terminal domains reveal a common motif. *Nat. Struct. Mol. Biol.* 12:1094–1100. http://dx.doi.org/10.1038/nsmb1017

Dyer, J.M., N.S. Savage, M. Jin, T.R. Zyla, T.C. Elston, and D.J. Lew. 2013. Tracking shallow chemical gradients by actin-driven wandering of the polarization site. *Curr. Biol.* 23:32–41. http://dx.doi.org/10.1016/j.cub.2012.11.014

Finger, F.P., T.E. Hughes, and P. Novick. 1998. Sec3p is a spatial landmark for polarized secretion in budding yeast. *Cell*. 92:559–571. http://dx.doi.org/10.1016/S0092-8674(00)80948-4

France, Y.E., C. Boyd, J. Coleman, and P.J. Novick. 2006. The polarity-establishment component Bem1p interacts with the exocyst complex through the Sec15p subunit. *J. Cell Sci.* 119:876–888. http://dx.doi.org/10.1242/jcs.02849

Guo, W., D. Roth, C. Walch-Solimena, and P. Novick. 1999. The exocyst is an effector for Sec4p, targeting secretory vesicles to sites of exocytosis. *EMBO J.* 18:1071–1080. http://dx.doi.org/10.1093/emboj/18.4.1071

Guo, W., F. Tamanoi, and P. Novick. 2001. Spatial regulation of the exocyst complex by Rho1 GTPase. *Nat. Cell Biol.* 3:353–360. http://dx.doi.org/10.1038/35070029

Harsay, E., and A. Bretscher. 1995. Parallel secretory pathways to the cell surface in yeast. *J. Cell Biol.* 131:297–310. http://dx.doi.org/10.1083/jcb.131.2.297

He, B., F. Xi, X. Zhang, J. Zhang, and W. Guo. 2007. Exo70 interacts with phospholipids and mediates the targeting of the exocyst to the plasma membrane. *EMBO J.* 26:4053–4065. http://dx.doi.org/10.1038/sj.emboj.7601834

Hsu, S.C., C.D. Hazuka, R. Roth, D.L. Foletti, J. Heuser, and R.H. Scheller. 1998. Subunit composition, protein interactions, and structures of the mammalian brain sec6/8 complex and septin filaments. *Neuron*. 20:1111–1122. http://dx.doi.org/10.1016/S0896-6273(00)80493-6

Hutagalung, A.H., J. Coleman, M. Pypaert, and P.J. Novick. 2009. An internal domain of Exo70p is required for actin-independent localization and mediates assembly of specific exocyst components. *Mol. Biol. Cell*. 20:153–163. http://dx.doi.org/10.1091/mbc.E08-02-0157

Kozminski, K.G., G. Alfaro, S. Dighe, and C.T. Beh. 2006. Homologues of oxysterol-binding proteins affect Cdc42p- and Rho1p-mediated cell polarization in *Saccharomyces cerevisiae*. *Traffic*. 7:1224–1242. http://dx.doi.org/10.1111/j.1600-0854.2006.00467.x

Liu, Y., J.J. Flanagan, and C. Barlowe. 2004. Sec22p export from the endoplasmic reticulum is independent of SNARE pairing. *J. Biol. Chem.* 279: 27225–27232. http://dx.doi.org/10.1074/jbc.M312122200

Longtine, M.S., D.J. DeMarini, M.L. Valencik, O.S. Al-Awar, H. Fares, C. De Virgilio, and J.R. Pringle. 1996. The septins: roles in cytokinesis and other processes. *Curr. Opin. Cell Biol.* 8:106–119. http://dx.doi.org/10.1016/S0955-0674(96)80054-8

Longtine, M.S., H. Fares, and J.R. Pringle. 1998. Role of the yeast Gin4p protein kinase in septin assembly and the relationship between septin assembly and septin function. *J. Cell Biol.* 143:719–736. http://dx.doi.org/10.1083/jcb.143.3.719

Mortensen, E.M., H. McDonald, J. Yates III, and D.R. Kellogg. 2002. Cell cycle-dependent assembly of a Gin4-septin complex. *Mol. Biol. Cell*. 13:2091–2105. http://dx.doi.org/10.1091/mbc.01-10-0500

Munson, M., and P. Novick. 2006. The exocyst defrocked, a framework of rods revealed. *Nat. Struct. Mol. Biol.* 13:577–581. http://dx.doi.org/10.1038/nsmb1097

Peterson, J., Y. Zheng, L. Bender, A. Myers, R. Cerione, and A. Bender. 1994. Interactions between the bud emergence proteins Bem1p and Bem2p and Rho-type GTPases in yeast. *J. Cell Biol.* 127:1395–1406. http://dx.doi.org/10.1083/jcb.127.5.1395

Pollard, T.D. 2010. A guide to simple and informative binding assays. *Mol. Biol. Cell*. 21:4061–4067. http://dx.doi.org/10.1091/mbc.E10-08-0683

Robinson, N.G., L. Guo, J. Imai, A. Toh-E, Y. Matsui, and F. Tamanoi. 1999. Rho3 of *Saccharomyces cerevisiae*, which regulates the actin cytoskeleton and exocytosis, is a GTPase which interacts with Myo2 and Exo70. *Mol. Cell. Biol.* 19:3580–3587.

Shen, D., H. Yuan, A. Hutagalung, A. Verma, D. Kümmel, X. Wu, K. Reinisch, J.A. McNew, and P. Novick. 2013. The synaptobrevin homologue Snc2p recruits the exocyst to secretory vesicles by binding to Sec6p. *J. Cell Biol.* 202:509–526. http://dx.doi.org/10.1083/jcb.201211148

Stalder, D., E. Mizuno-Yamasaki, M. Ghassemian, and P.J. Novick. 2013. Phosphorylation of the Rab exchange factor Sec2p directs a switch in regulatory binding partners. *Proc. Natl. Acad. Sci. USA*. 110:19995–20002. http://dx.doi.org/10.1073/pnas.1320029110

TerBush, D.R., T. Maurice, D. Roth, and P. Novick. 1996. The Exocyst is a multiprotein complex required for exocytosis in *Saccharomyces cerevisiae*. *EMBO J.* 15:6483–6494.

Wu, H., C. Turner, J. Gardner, B. Temple, and P. Brennwald. 2010. The Exo70 subunit of the exocyst is an effector for both Cdc42 and Rho3 function in polarized exocytosis. *Mol. Biol. Cell*. 21:430–442. http://dx.doi.org/10.1091/mbc.E09-06-0501

Yamaguchi, Y., K. Ota, and T. Ito. 2007. A novel Cdc42-interacting domain of the yeast polarity establishment protein Bem1. Implications for modulation of mating pheromone signaling. *J. Biol. Chem.* 282:29–38. http://dx.doi.org/10.1074/jbc.M609308200

Yamashita, M., K. Kurokawa, Y. Sato, A. Yamagata, H. Mimura, A. Yoshikawa, K. Sato, A. Nakano, and S. Fukai. 2010. Structural basis for the Rho- and phosphoinositide-dependent localization of the exocyst subunit Sec3. *Nat. Struct. Mol. Biol.* 17:180–186. http://dx.doi.org/10.1038/nsmb.1722

Yeaman, C., K.K. Grindstaff, and W.J. Nelson. 2004. Mechanism of recruiting Sec6/8 (exocyst) complex to the apical junctional complex during polarization of epithelial cells. *J. Cell Sci.* 117:559–570. http://dx.doi.org/10.1242/jcs.00893

Zajac, A., X. Sun, J. Zhang, and W. Guo. 2005. Cyclical regulation of the exocyst and cell polarity determinants for polarized cell growth. *Mol. Biol. Cell*. 16:1500–1512. http://dx.doi.org/10.1091/mbc.E04-10-0896

Zhang, X., E. Bi, P. Novick, L. Du, K.G. Kozminski, J.H. Lipschutz, and W. Guo. 2001. Cdc42 interacts with the exocyst and regulates polarized secretion. *J. Biol. Chem.* 276:46745–46750. http://dx.doi.org/10.1074/jbc.M107464200

Zhang, X., K. Orlando, B. He, F. Xi, J. Zhang, A. Zajac, and W. Guo. 2008. Membrane association and functional regulation of Sec3 by phospholipids and Cdc42. *J. Cell Biol.* 180:145–158. http://dx.doi.org/10.1083/jcb.200704128